A human coronavirus OC43 variant harboring persistence-associated mutations in the S glycoprotein differentially induces the unfolded protein response in human neurons as compared to wild-type virus

Dominique J. Favreau, Marc Desforges, Julien R. St-Jean, Pierre J. Talbot *

Laboratory of Neuroimmunovirology, INRS-Institut Armand-Frappier,531 boulevard des Prairies, Laval, Québec, Canada H7V 1B7

ARTICLE INFO

ABSTRACT

We have reported that human respiratory coronavirus OC43 (HCoV-OC43) is neurotropic and neuroinvasive in humans and mice, and that neurons are the primary target of infection in mice, leading to neurodegenerative disabilities. We now report that an HCoV-OC43 mutant harboring two persistence-associated S glycoprotein point mutations (H183R and Y241H), induced a stronger unfolded protein response (UPR) and translation attenuation in infected human neurons. There was a major contribution of the IRE1/XBP1 pathway, followed by caspase-3 activation and nuclear fragmentation, with no significant role of the ATF6 and eIF2-alpha/ATF4 pathways. Our results show the importance of discrete molecular viral S determinants in virus–neuronal cell interactions that lead to increased production of viral proteins and infectious particles, enhanced UPR activation, and increased cytotoxicity and cell death. As this mutant virus is more neurovirulent in mice, our results also suggest that two mutations in the S glycoprotein could eventually modulate viral neuropathogenesis.

© 2009 Elsevier Inc. All rights reserved.

Introduction

Human coronaviruses (HCoV) are enveloped positive-stranded RNA viruses and known respiratory pathogens (Talbot et al., 2008) with neurotropic and neuroinvasive properties (Arbour et al., 2000; Bonavia et al., 1997). Indeed, we reported that the OC43 strain (HCoV-OC43) could infect and persist in human neural cell lines (Arbour et al., 1999), and infect primary human and murine central nervous system (CNS) cultures (Bonavia et al., 1997; Jacomy et al., 2006). Moreover, neurons were the main target of infection in the murine CNS (Jacomy et al., 2006), as well as in human co-cultures of neurons and astrocytes (M. Desforges and P.J. Talbot, unpublished data). Furthermore, HCoV-OC43 induced a chronic encephalitis in susceptible mice (Jacomy et al., 2006), HCoV RNA was detected in human brains (Arbour et al., 2000) and HCoV-OC43 was associated with acute disseminated encephalomyelitis (Yeh et al., 2004). Considering that murine hepatitis virus, MHV, the murine counterpart of HCoV-OC43, causes neurological disease in mice (Buchmeier et al., 1987), we hypothesized that HCoV-OC43 might be associated with some human neurological diseases.

In several neurodegenerative diseases, such as Alzheimer's disease (AD) (Imaizumi et al., 2001) and Parkinson's disease (PD) (Imai et al., 2000), neuronal death has been linked to endoplasmic reticulum (ER) stress. Defects in neuronal ER function can lead to accumulation of misfolded proteins and activate the unfolded protein response (UPR), usually leading to the recovery of ER homeostasis (Ron and Walter, 2007). On the other hand, impaired UPR activation was recently associated with human neurological diseases (Antony et al., 2007; Lindholm et al., 2006; Paschen, 2003).

So far, three pathways have been identified to play a role in the UPR, namely ATF6, PERK/eIF2-alpha and IRE1/XBP1 (Ron and Walter, 2007). These pathways are activated when the UPR regulatory protein, GRP78, is delocalized from its inhibitory sites on the ER-stress-sensor proteins, ATF6, PERK and IRE1 (Ron and Walter, 2007).

ATF6 is a major transcriptional factor that leads to upregulation of chaperones involved in the recovery of ER protein folding capacity (Ron and Walter, 2007). PERK is activated following homodimerization and plays a major role in the phosphorylation of the translation initiation factor eIF2-alpha (Shi et al., 1998). IRE1 is an endoribonuclease and kinase which undergoes oligomerization and autophosphorylation, leading to its activation following UPR induction (Tirasophon et al., 1998; Tirasophon et al., 2000; Yoshida et al., 2001). IRE1 is responsible for the unconventional splicing of Xbp1(u) mRNA by excising an 26-nucleotide intron, yielding the Xbp1(s) mRNA form (Yoshida et al., 2001). Xbp1(s) is translated into a transcription factor, XBP1, which translocates to the nucleus (Yoshida et al., 2001). XBP1 induces the expression of genes related to proteasomal degradation of proteins (Yamamoto et al., 2004). XBP1 may also promote the expression of the genes Grp94, an ER chaperone (Yamamoto et al., 2004), and Chop (Lee et al., 2003). XBP1 is also

* Corresponding author. Fax: +1 450 686 5501.
  E-mail address: pierre.talbot@iaf.inrs.ca (P.J. Talbot).

known to solely induce the expression of P58-ipk, an inhibitor of PERK kinase activity (Lee et al., 2003), preventing its ability to phosphorylate eIF2-alpha.

The UPR has been shown to be induced by a number of viruses, such as human cytomegalovirus (Isler et al., 2005), herpes simplex virus (Cheng et al., 2005), hepatitis C virus (Tardif et al., 2002), Japanese encephalitis virus (Yu et al., 2006), Borna disease virus (Williams and Lipkin, 2006), Dengue virus (Umareddy et al., 2007), SARS-CoV (Chan et al., 2006) and MHV (Bechill et al., 2008). Various viruses have evolved different strategies to modulate its activation and/or benefit from it. Interestingly, the S proteins of the coronaviruses MHV (Versteeg et al., 2007) and SARS-CoV (Chan et al., 2006) were shown to induce UPR within cells. Even though the involvement of the coronavirus S protein in neurovirulence (Phillips et al., 1999) and the UPR in neurological diseases (Lindholm et al., 2006) have been suggested, no studies have, to our knowledge, been performed to identify specific amino acid residues within the S protein which would differ between coronavirus variants and correlate with an increased neurovirulence and UPR activation.

Consequently, UPR activation within human neurons following infection by HCoV-OC43 was examined in the human neuronal models, the NT2-N (Pleasure and Lee, 1993) and the LA-N-5 (Hill and Robertson, 1998), in order to study pathways that might ultimately be involved in coronavirus-induced neurological diseases. Two HCoV-OC43 point mutations that reproducibly appeared upon persistent infection of human neural cell lines (H183R and Y241H) were introduced into an infectious cDNA clone (St-Jean et al., 2006) and generated an HCoV-OC43 variant which induced an increased UPR within infected human neurons, an interesting fact as this variant showed enhanced neurovirulence in mice (H. Jacomy and P. J. Talbot, submitted for publication).

Results

Human differentiated neuronal cell lines were susceptible to a productive HCoV-OC43 infection

As we have previously shown that neurons are the main target of HCoV-OC43 infection in the mouse CNS (Jacomy and Talbot, 2003) and in NT2-N/human primary astrocytes co-cultures (M. Desforges and P. J. Talbot, unpublished data), we sought to study the early cellular events occurring in human neurons after HCoV-OC43 infection. First, we evaluated the susceptibility of the two well-characterized differentiated human neuronal cell lines NT2-N (Pleasure and Lee, 1993) and LA-N-5 (Hill and Robertson, 1998) to HCoV-OC43 (ATCC strain) infection. Immunofluorescence analysis confirmed the neuronal nature of the cells, as revealed by the detection of specific neuronal markers, NFM for LA-N-5 and β-tubIII for NT2-N (Fig. 1A, panels a and b), and their susceptibility to HCoV-OC43 infection was demonstrated by the detection of viral antigens (Fig. 1A, panels c and d). Furthermore, the infection was shown to be productive, as demonstrated by the increase in infectious HCoV-OC43 progeny virions in cell culture medium over a period of 72 h post-infection (Fig. 1B).

Infection of human neurons by HCoV-OC43 modulated the expression of 275 genes

In order to study the early cellular events occurring in human neurons following HCoV-OC43 infection, we investigated the transcriptomic profile of neurons at 24, 48 and 72 h post-infection, as compared to mock-infected cells. Total RNA of NT2-N cells was extracted and linearly amplified mRNAs were hybridized on microarray chips representing 22,000 human transcripts. Considering that Cy3-CTP and Cy5-CTP do not incorporate at the same rate during the amplification stage, we performed duplicate microarray experiments
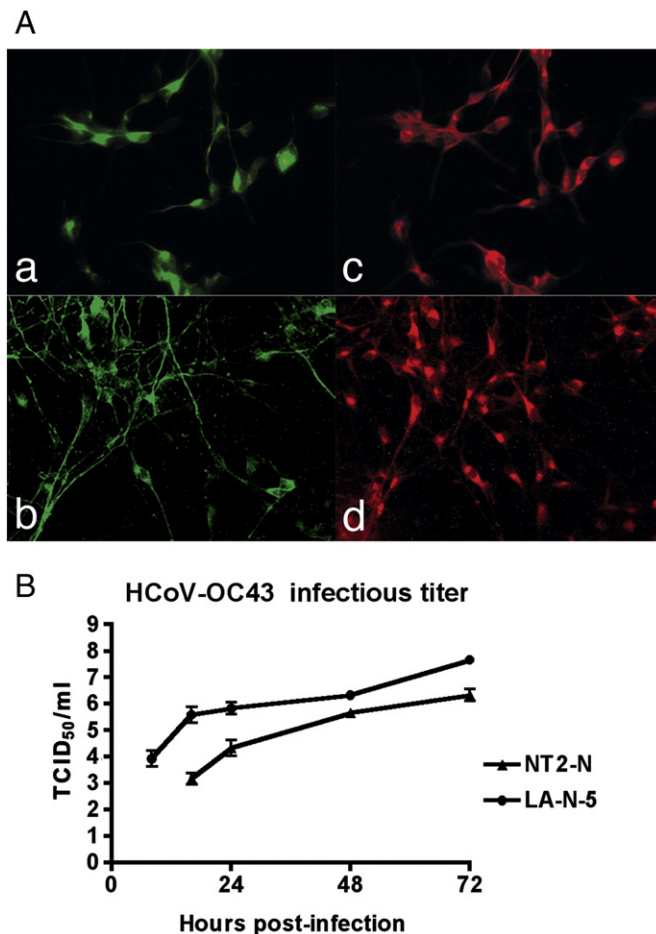

Fig. 1. Human differentiated neuronal cell lines were susceptible to a productive HCoV-OC43 infection. (A) Immunofluorescence on cell lines differentiated into human neurons, LA-N-5 (panels a and c) and NT2-N (panels b and d), using specific neuronal markers NFM (panel a) and β-tub isoform III (panel b), or detection of HCoV-OC43 (panels c and d). (B) Production of infectious HCoV OC43 particles in supernatants of infected LA-N-5 and NT2-N cell lines differentiated into human neurons.

in dye-swap to prevent label-bias in analysis (Tseng et al., 2001). Results of internal chip controls showed a correlation of more than 95% compared to their expected modulation, confirming the reliability of our modulation results (data not shown). We identified a total of 275 genes, the expression of which was significantly modulated at 24, 48 and/or 72 h post-infection, in at least two independent infections, with a maximum p-value of 0.05. The transcriptomic profile showed a diversity in the modulation of expression of genes that we grouped into nine major cellular functional groups (Fig. 2).

Infection of both NT2-N and LA-N-5 human neurons by HCoV-OC43 led to the modulation of expression of a subset of genes related to the unfolded protein response

Analysis of the transcriptomic profile revealed a modulation of expression of several genes in the Biosynthesis and Degradation functional group (Fig. 2) that are related to the unfolded protein response (UPR), which can be activated by different types of stress, including viral infection. The UPR occurring in human neurons is also associated with various neurodegenerative diseases, such as Alzheimer's disease (Imaizumi et al., 2001) and Parkinson's disease (Imai et al., 2000). Moreover, some studies also indicated that ER stress induced in neurons might underlie the neuropathological mechanisms leading to neuronal injury (Paschen, 2001). Therefore, we sought to analyze the activation of the three UPR pathways, namely ATF6, PERK/eIF2-alpha and IRE1/XBP1.

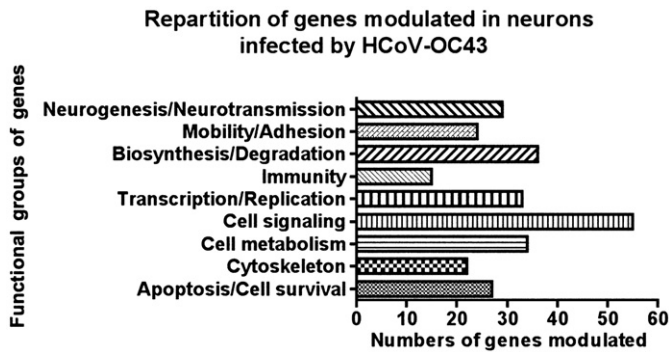## Repartition of genes modulated in neurons infected by HCoV-OC43

Fig. 2. Distribution of the 275 genes which expression was modulated in the human NT2-N neuronal cell line at 24, 48 or 72 h after infection with HCoV-OC43, grouped into nine major cellular functional groups. Neurogenesis/neurotransmission: 29 genes; mobility/adhesion: 24 genes; biosynthesis/degradation: 36 genes; immunity: 15 genes; transcription/replication: 33 genes; cell signaling: 55 genes; cell metabolism: 34 genes; cytoskeleton: 22 genes; apoptosis/cell survival: 27 genes.

First, the modulation of expression of genes related to the UPR revealed by our microarray experiments, was confirmed by quantitative PCR in both NT2-N and LA-N-5 cells. Total RNA was reverse-transcribed before performing real-time quantitative PCR, using primers specific to each gene of interest (Supplementary data 1). Our results showed a high correlation between the NT2-N and LA-N-5 neuronal models in the modulation of expression of UPR-related genes following HCoV-OC43 infection (Table 1). The degree of induction (fold-induction) in the expression of the Atf4, Erdj3, Erdj4, Gadd34, Grp78 and Grp94 genes clearly indicated a significant similarity between the response of both NT2-N and LA-N-5 cells, establishing a relevant consistency between the two models (Table 1). Moreover, even though there were some differences in the degree of induction of gene expression in the two cell lines for the Chop, Edem, Herp, P58-ipk and Xbp1 genes, an upregulation was always observed over the time-course of HCoV-OC43 infection (Table 1). Indeed, the trend in the modulation of expression of these genes followed the same pattern in both NT2-N and LA-N-5 cells, which again revealed a consistency in the state of activation of the underlying pathways.

A recombinant HCoV-OC43 used to study the impact of the S glycoprotein on UPR activation showed increased viral replication within infected neurons but no difference in the kinetics of replication in cell culture, as compared to HCoV-OC43 wild-type

Previous studies have reported that the S protein of coronaviruses can alone induce the UPR within cells (Chan et al., 2006; Versteeg et

al., 2007). Consequently, we sought to determine whether a HCoV-OC43 variant harboring mutations within the S protein related to enhanced neurovirulence in mice (H. Jacomy and P. J. Talbot, submitted for publication), could differentially induce the UPR in human neurons, compared to the so-called HCoV-OC43 wild-type, which we obtained several years ago from the ATCC. Two point mutations (H183R and Y241H) identified in the S protein of a HCoV-OC43 variant obtained from persistently infected human neural cell lines were introduced into the HCoV-OC43 genome using our full-length cDNA clone pBAC-OC43^{FL} (St-Jean et al., 2006), yielding a recombinant virus which we designated HCoV-OC43 rOC/$U_{S183-241}$. Before analyzing the effects of these mutations on UPR activation, we sought to determine whether both viruses showed similar kinetics of replication and dissemination in cell culture. The production of extra- and intra-cellular infectious viral particles was evaluated at 4, 8, 12, 16, 20, 24, 48 and 72 h post-infection. No differences in extra-cellular infectious titers were observed between HCoV-OC43 wild-type and HCoV-OC43 rOC/$U_{S183-241}$ (Fig. 3A, left panel). However, a significant increase in the production of intra-cellular infectious viral particles was noted for HCoV-OC43 rOC/$U_{S183-241}$ as compared to HCoV-OC43 wild-type (Fig. 3A, right panel). Moreover, cells infected by HCoV-OC43 rOC/$U_{S183-241}$ produced more viral S proteins, as shown by flow cytometry at 24 h post-infection (Fig. 3C) and by immunofluorescence revealed by microscopic observation (Fig. 3B). We then assessed the percentage of infected cells at 4, 16 and 24 h post-infection by flow cytometry and found that there were no differences between the two viruses in their spread in the neuronal cultures, as the percentage of infected cells was not significantly different (Fig. 3D). Globally, our data indicate that the two viruses have the same capacity to release infectious particles in the cell medium and that their kinetics of dissemination within neuronal cultures were comparable. However, we did observe a significant increase in the amount of viral proteins and infectious viral particles within cells infected by the variant HCoV-OC43 rOC/$U_{S183-241}$.

The ATF6 pathway in human neurons is functional and was activated by thapsigargin but not by infection with HCoV-OC43 wild-type and the HCoV-OC43 rOC/$U_{S183-241}$ variant

In order to decipher which branches of the UPR were activated after infection, the ATF6 pathway was first examined as it is involved in the expression of ER chaperones, leading to an increase of protein folding capacity of the cell. During the course of UPR, ATF6 is cleaved within the Golgi, leading to the appearance of ATF6 transcriptional factors, which are translocated to the nucleus where they mainly bind cis-acting ER stress-response element (ERSE) (Okada et al., 2002). As

Table 1
Time-course of gene expression related to the unfolded protein response within human neurons infected by HCoV-OC43.[a]

Gene name	Common gene name	Gene ID	24 h post-infection			48 h post-infection			72 h post-infection		
			Microarray NT2-N	qPCR NT2-N	qPCR LA-N-5	Microarray NT2-N	qPCR NT2-N	qPCR LA-N-5	Microarray NT2-N	qPCR NT2-N	qPCR LA-N-5
ATF4	ATF4	NM_001675	–[b]	1.12	1.11	3.38	3.47	1.63	2.49	2.58	3.25
DDIT3	CHOP	NM_004083	–[b]	1.30	1.54	3.69	4.59	6.38	2.22	5.10	12.24
EDEM1	EDEM1	NM_014674.1	–[b]	1.20	1.13	–[b]	5.54	4.56	–[b]	5.00	15.38
DNAJB11	Erdj3	NM_016306	–[b]	1.14	1.13	3.49	3.20	1.91	3.02	2.64	4.22
DNAJB9	Erdj4	NM_012328	2.07	1.34	1.16	5.02	5.45	2.73	3.25	4.63	4.42
PPP1R15A	GADD34	NM_014330.3	–[b]	1.06	1.13	–[b]	3.02	3.14	–[b]	3.20	7.00
HSPA5	GRP78	NM_005347.2	–[b]	0.75	0.95	–[b]	1.58	1.23	–[b]	1.18	1.72
HSP90B1	GRP94	NM_003299.1	–[b]	1.11	1.03	6.56	3.59	2.18	4.50	3.05	3.77
HERPDU1	HERPDU1	NM_014685	2.08	1.55	1.87	8.88	5.83	9.06	4.23	5.13	35.10
DNAJC3	P58-IPK	NM_006260	–[b]	1.54	1.16	3.56	8.09	15.85	–[b]	8.51	17.51
XBP1	XBP1(s)	NM_001079539.1	–[b]	2.17	2.46	–[b]	13.99	15.56	–[b]	5.24	26.35

[a] Numbers represent the degree of induction (fold-induction) of each gene in HCoV-OC43 infected NT2-N or LA-N-5 cells, at the indicated times post-infection, as revealed by either microarray or real-time quantitative PCR (qPCR).
[b] Gene is not significantly modulated according to microarray results.
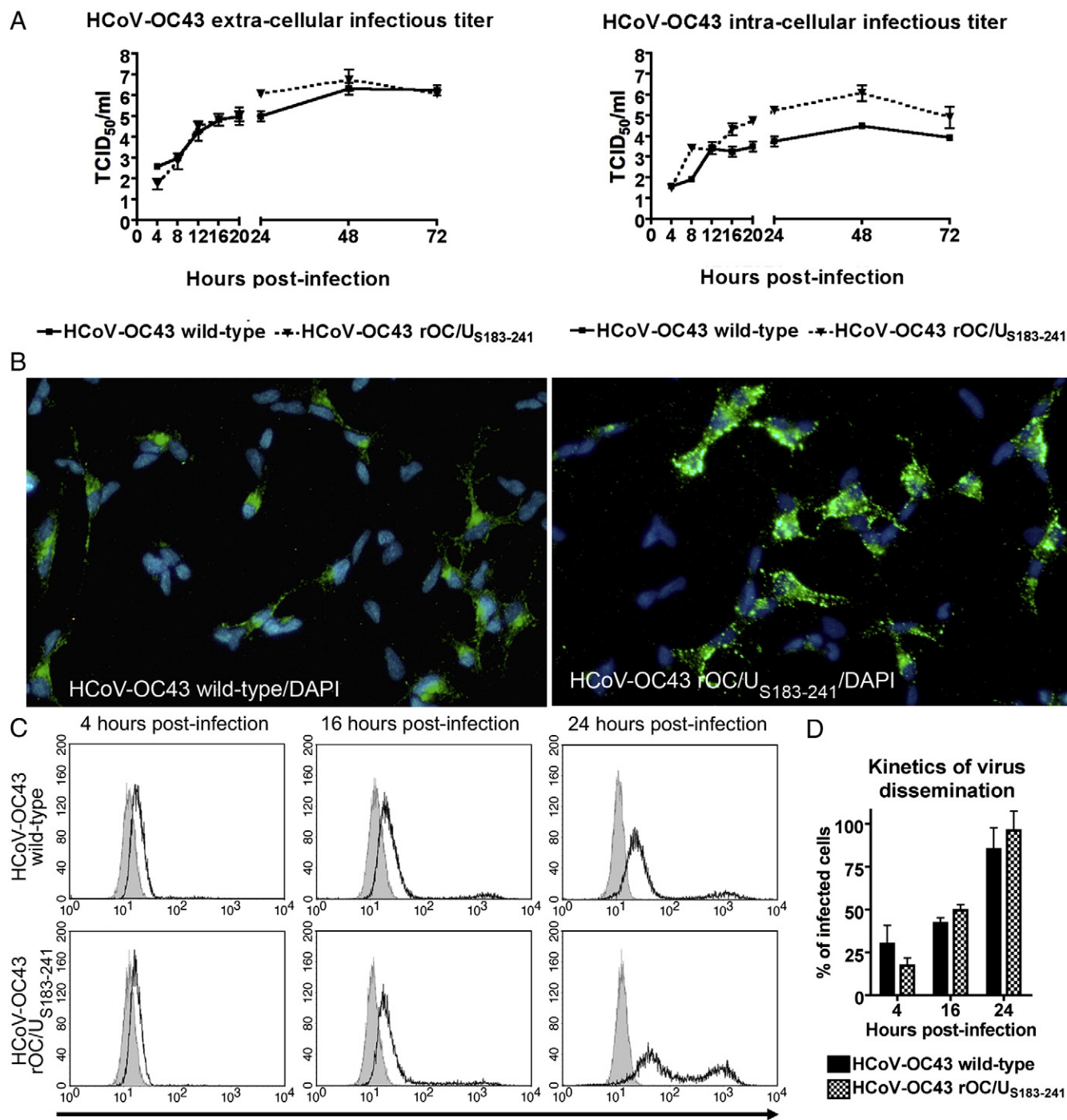
Fig. 3. A recombinant HCoV-OC43 with two point mutations within the S protein showed increased viral replication within infected neurons but no difference in the kinetics of replication in cell culture compared to HCoV-OC43 wild-type. LA-N-5 cells were infected with HCoV-OC43 wild-type or HCoV-OC43 rOC/U$_{S183-241}$ variant for 4, 8, 12, 16, 20, 24, 48 or 72 h. (A) Production of viral infectious particles. Supernatants and cells were separately harvested and titers of extra-and intra-cellular viral infectious particles were assayed. (B) Detection of viral antigens within neurons infected by HCoV-OC43 wild-type or HCoV-OC43 rOC/U$_{S183-241}$. Merged images of immunofluorescence of LA-N-5 differentiated into human neurons infected with HCoV-OC43 wild-type (left panel) or HCoV-OC43 rOC/U$_{S183-241}$ (right panel) showing HCoV-OC43 antigens (green) and DAPI (blue). (C) Kinetics of infection of neurons. Neurons were infected and, at the indicated times post-infection, fixed, permeabilized, labeled with antibody directed against HCoV-OC43 or HCoV-229E (isotype control) and labeled with secondary antibody AlexaFluor 488 anti-mouse. Grey area represent cells labeled with isotype control antibody and white area represent cells labeled with HCoV-OC43 antibody. (D) Percentage of infected neurons. Percentage of cells labeled with HCoV-OC43 antibody were quantified considering the background established with cells labeled with HCoV-229E isotype control antibody.

the Grp78 gene is a major target of ATF6 and a central effector of the UPR, its expression was assessed by quantitative real-time PCR to determine the degree of activation of the ATF6 pathway. Infection of neurons with HCoV-OC43 wild-type did not result in any significant modulation of the expression of Grp78 (Fig. 4A). On the other hand, infection with HCoV-OC43 rOC/U$_{S183-241}$ did result in a 3-fold transient increase of Grp78 expression (Fig. 4A). The level of

expression of the corresponding GRP78 protein was examined by Western blotting but no significant difference in the expression of the GRP78 protein between mock-infected cells and infected cells by either HCOV-OC43 wild-type or HCoV-OC43 rOC/U$_{S183-241}$ was detected (Fig. 4B). Thapsigargin-treated cells were used a positive control and did demonstrate the capacity of the neuronal cells to express GRP78 following activation of the UPR (Fig. 4B). As Grp78 is

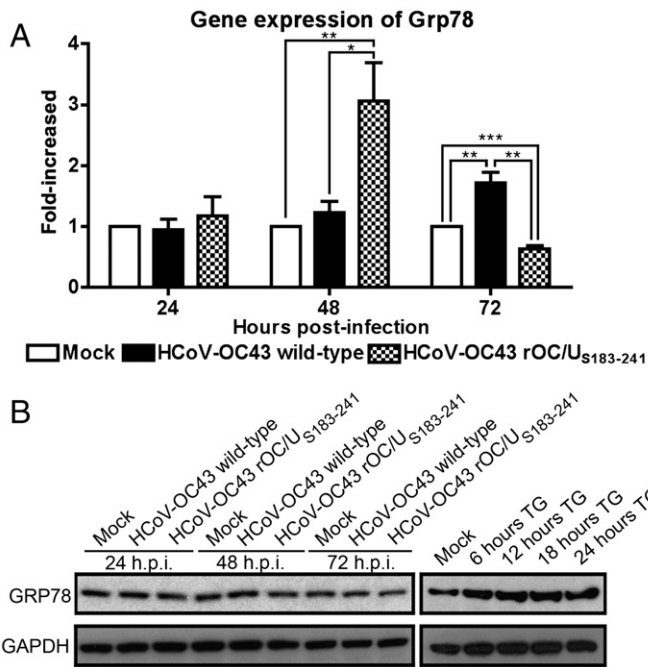infection, which correlates with our observations of intra-cellular infectious viral titers (Fig. 3A), immunofluorescence (Fig. 3B) and flow cytometry (Figs. 3C and D). Thapsigargin-treated cells served as a positive control of protein synthesis inhibition, demonstrating that repression of mRNA translation could indeed occur in neurons. Staining of the gel with Coomassie blue was used as a loading control (data not shown). Altogether, these results suggest that translational repression observed after 24 h post-infection was not a consequence
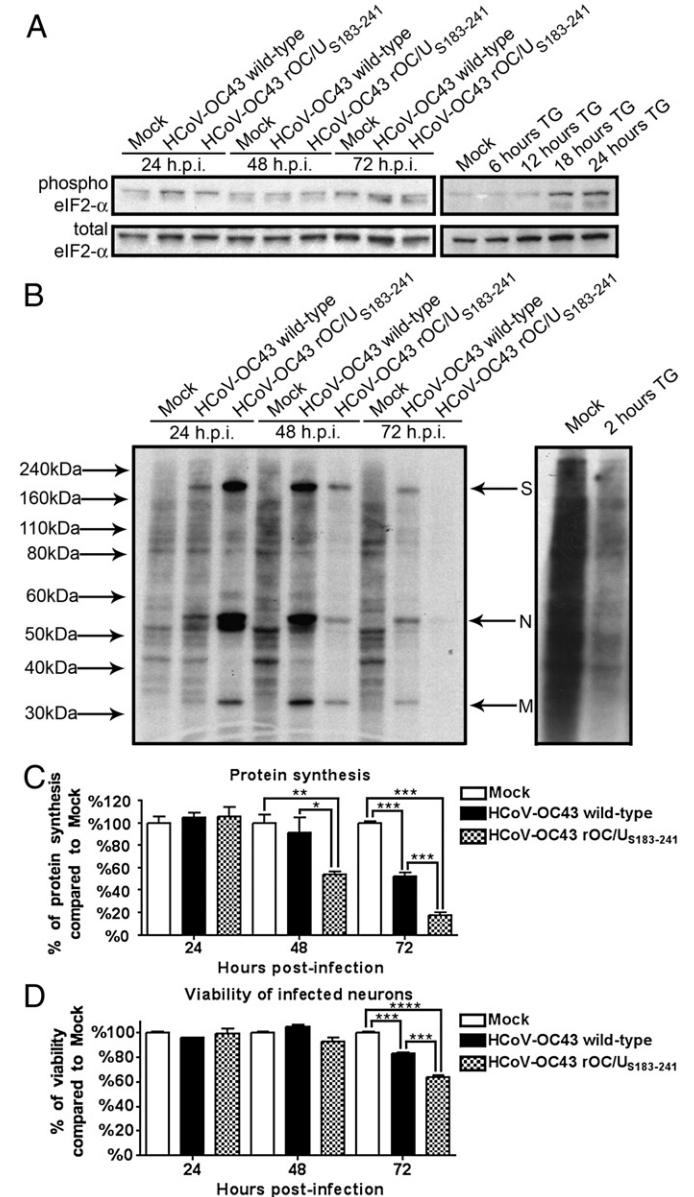
Fig. 4. The ATF6 pathway was not activated following infection of human neurons with HCoV-OC43 wild-type and HCoV-OC43 rOC/U$_{S183-241}$ variant. LA-N-5 cells were infected with HCoV-OC43 wild-type or HCoV-OC43 rOC/U$_{S183-241}$ variant for 24, 48 or 72 h, or incubated in presence of 2 μM of thapsigargin for 6, 12, 18 or 24 h. (A) Grp78 gene expression analysis. Total RNA extracted was reverse-transcribed and mRNA expression was evaluated by quantitative PCR compared to mock-infected cells. Gapdh expression was used for normalization. Statistical significance: *$p < 0.05$; **$p < 0.01$; ***$p < 0.0001$. (B) GRP78 protein expression analysis. Whole cell lysates were subjected to Western blot analysis using antibody directed against GRP78. GAPDH served as a loading control. Thapsigargin-treated samples served as a positive control.

the major gene modulated by the ATF6 pathway of the UPR, our data indicate that the ATF6 pathway is functional in the LA-N-5 cells but that it did not play a significant role in the UPR induced by infection with either virus.

Infection of human neurons with the HCoV-OC43 rOC/U$_{S183-241}$ variant led to a stronger protein synthesis attenuation compared to infection with HCoV-OC43 wild-type

Another UPR pathway potentially activated following ER stress is PERK/eIF2-alpha. The ER sensor PERK induces the phosphorylation of the eIF2-alpha translation initiation factor in order to reduce total protein synthesis. As other coronaviruses are known to induce eIF2-alpha phosphorylation and attenuation of protein synthesis (Bechill et al., 2008), we investigated whether HCoV-OC43 wild-type or HCoV-OC43 rOC/U$_{S183-241}$ could do the same. Western blot analysis showed that eIF2-alpha was only transiently phosphorylated at 24 h post-infection by both viruses and that the phosphorylation state of eIF2-alpha then returned to its basal level within 48 h post-infection, as compared to mock-infected cells (Fig. 5A). The use of thapsigargin-treated cells indicated that eIF2-alpha could indeed be phosphorylated in neurons during the activation of the UPR (Fig. 5A).

The total neuronal translational activity was determined by [^{35}S] cystein/methionine incorporation into proteins to determine whether the transient phosphorylation of eIF2-alpha could lead to an attenuation of mRNA translation. Strikingly, no significant decrease in protein translation was observed following infection by both viruses at 24 h post-infection, as compared to mock-infected cells, as revealed by autoradiographic gel and quantified after TCA precipitation (Fig. 5B and 5C). The three intense bands present only in infected-cells, which likely correspond to the viral S, N and M proteins, showed a stronger expression in cells infected by HCoV-OC43 rOC/U$_{S183-241}$ at 24 h post-

Fig. 5. Infection of human neurons with the HCoV-OC43 rOC/U$_{S183-241}$ variant led to a stronger protein translation attenuation, as compared to HCoV-OC43 wild-type. The LA-N-5 cells were infected with HCoV-OC43 wild-type or HCoV-OC43 rOC/U$_{S183-241}$ for 24, 48 or 72 h, or incubated in the presence of 2 μM of thapsigargin for 2 h. (A) eIF2-alpha phosphorylation-state analysis. Whole cell lysates were subjected to Western blot analysis using antibody directed against Ser52-phosphorylated eIF2-alpha. Total eIF2-alpha served as a loading control. Thapsigargin-treated samples served as a positive control. (B and C) Protein synthesis analysis. Cell cultures were starved for cysteine and methionine for 30 min, then incubated with ^{35}S-radiolabeled cysteine/methionine for 15 min and harvested. Whole cell lysates were assayed for cpm (C) counts and resolved on a 4–12% polyacrylamide gel (B). Thapsigargin-treated cells served as a translational shutoff control. (D) Cell viability assay. Cell cultures were incubated with the MTS/PMS solution and absorbance was read at 492 nm. Cell viability is expressed as a relative percentage compared to mock-infected cells. Statistical significance: *$p < 0.05$; **$p < 0.001$; ***$p < 0.0001$; ****$p < 0.000001$.

A
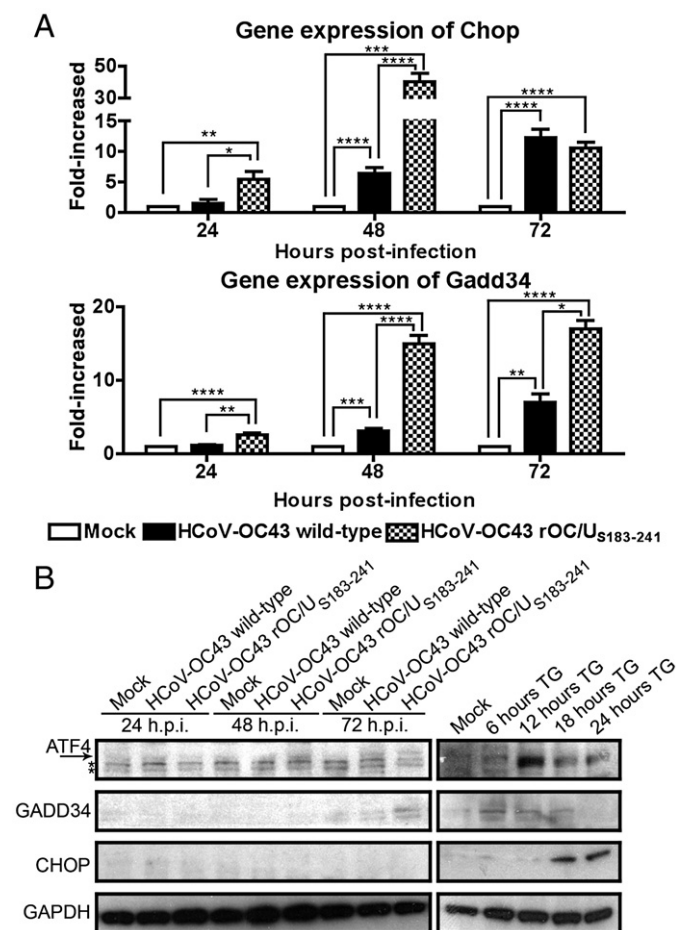

Gene expression of Chop

Gene expression of Gadd34

☐ Mock ■ HCoV-OC43 wild-type ▨ HCoV-OC43 rOC/U$_{S183-241}$

B

the ATF4 protein regulates the expression of the Gadd34 and Chop genes, respectively involved in the dephosphorylation of eIF2-alpha (Novoa et al., 2001) and in the induction of apoptosis (Matsumoto et al., 1996; Zinszner et al., 1998), the potential modulation of expression of these genes was analyzed by quantitative PCR. Our results revealed clear differences in the kinetics of induction of the Chop gene expression after infection with HCoV-OC43 wild-type or HCoV-OC43 rOC/U$_{S183-241}$ (Fig. 6A). Chop was strongly induced at 48 h post-infection by HCoV-OC43 rOC/U$_{S183-241}$ and its expression decreased at 72 h post-infection. On the other hand, infection with HCoV-OC43 wild-type led to a constantly increasing level of the Chop gene up to 72 h post-infection, but to a lower level than for HCoV-OC43 rOC/U$_{S183-241}$.
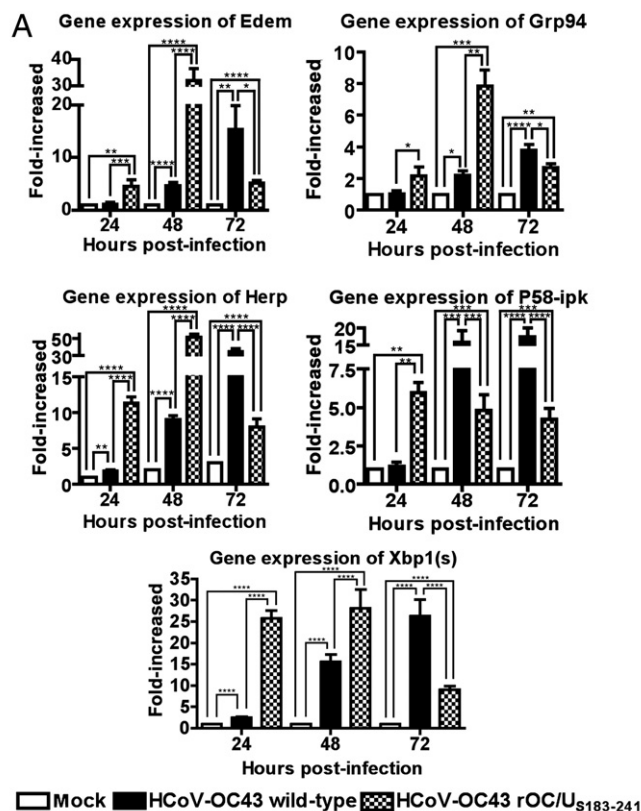
A

Gene expression of Edem

Gene expression of Grp94

Gene expression of Herp

Gene expression of P58-ipk

Gene expression of Xbp1(s)

☐ Mock ■ HCoV-OC43 wild-type ▨ HCoV-OC43 rOC/U$_{S183-241}$

B

Fig. 6. Infection of human neurons with the HCoV-OC43 rOC/U$_{S183-241}$ variant strongly induced expression of genes Chop and Gadd34, compared to HCoV-OC43 wild-type. The LA-N-5 cells were infected with HCoV-OC43 wild-type or HCoV-OC43 rOC/U$_{S183-241}$ for 24, 48 or 72 h, or incubated in presence of 2 μM of thapsigargin for 6, 12, 18 or 24 h. (A) Chop and Gadd34 gene expression analysis. Total RNA was extracted and reverse-transcribed and mRNA expression was evaluated by quantitative PCR compared to mock-infected. Gapdh expression was used for normalization. Statistical significance: *$p<0.05$; **$p<0.01$; ***$p<0.001$; ****$p<0.0001$. (B) ATF4, CHOP and GADD34 protein expression analysis. Whole cell lysates were subjected to Western blot analysis using antibody directed against ATF4, CHOP or GADD34. GAPDH served as a loading control. Thapsigargin-treated samples served as a positive control. *Non-specific bands on ATF4 Western blot.

of an activated PERK/eIF2-alpha pathway. Moreover, translation attenuation started only at 72 h post-infection for HCoV-OC43 wild-type, in comparison to 48 h post-infection for HCoV-OC43 rOC/U$_{S183-241}$. These results demonstrate that only two point mutations in the S protein of HCoV-OC43 can result in a different kinetics of total protein synthesis attenuation following infection.

In order to confirm that the observed protein synthesis attenuation was not a consequence of cell death, cell viability was assessed. Data at 48 and 72 h post-infection showed that this attenuation preceded the loss of cell viability (Figs. 5C and D), suggesting that the reduction of protein synthesis preceded cell death and therefore was not only its consequence.

Infection of human neurons with the HCoV-OC43 rOC/U$_{S183-241}$ variant led to a stronger activation of the expression of genes Chop and Gadd34, compared to infection with HCoV OC43 wild-type

Considering the transient phosphorylation of eIF2-alpha (Fig. 5A), the activation of related UPR factors was examined. Atf4 mRNA is known to be preferentially translated into a transcription factor when eIF2-alpha is phosphorylated (Harding et al., 2000). Considering that

Fig. 7. The IRE1/XBP1 pathway was rapidly activated following infection of human neurons with the HCoV-OC43 rOC/U$_{S183-241}$ variant, as compared to HCoV-OC43 wild-type. The LA-N-5 cells were infected with HCoV-OC43 wild-type or HCoV-OC43 rOC/U$_{S183-241}$ for 24, 48 or 72 h, or incubated in presence of 2 μM of thapsigargin for 6, 12, 18 or 24 h. (A) Xbp1(s), Xbp1(u)(s), Grp94, Edem, Herp and P58-ipk gene expression analysis. Total RNA was extracted and reverse-transcribed and mRNA expression was evaluated by quantitative PCR compared to mock-infected. Gapdh expression was used for normalization. Statistical significance: *$p<0.05$; **$p<0.01$; ***$p<0.001$; ****$p<0.0001$. (B) GRP94 protein expression analysis. Whole cell lysates were subjected to Western blot analysis using antibody directed against GRP94. GAPDH served as a loading control. Thapsigargin-treated samples served as a positive control.
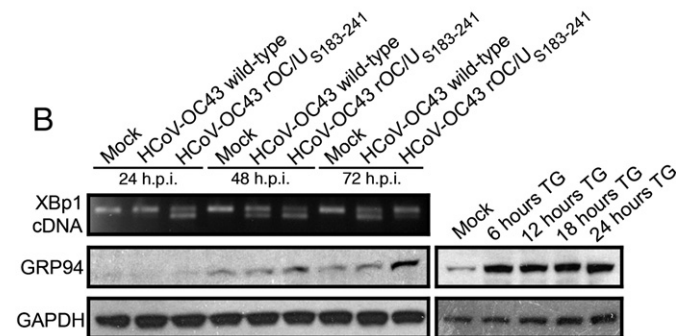
Even though Gadd34 expression is also considered to be regulated by ATF4, its expression followed a different kinetics. Both HCoV-OC43 wild-type and HCoV-OC43 rOC/U$_{S183-241}$ induced the upregulation of Gadd34, which expression gradually increased up to 72 h post-infection (Fig. 6A), with a more pronounced induction after infection by HCoV-OC43 rOC/U$_{S183-241}$. Even though there was no significant level of phosphorylated eIF2-alpha at 48 and 72 h post-infection (Fig. 5A), the level of expression of the ATF4 protein was evaluated to determine whether the expression of the Chop and Gadd34 genes could be linked to this protein. We were not able to detect any expression of the ATF4 protein following infection by both viruses (Fig. 6B). The level of expression of the CHOP and GADD34 proteins was then assessed to verify whether the observed increase in expression of the corresponding gene led to an increase in the amount of the corresponding protein. Strikingly, no increase in the CHOP protein was observed even though we observed a 50-fold increase in gene expression at 48 h post-infection by HCoV OC43 rOC/U$_{S183-241}$, compared to mock-infected cells. On the other hand, a slight increase in the amount of GADD34 protein could be detected at 72 h after infection by HCoV-OC43 rOC/U$_{S183-241}$. Thapsigargin-treated cells were used as a positive control to demonstrate that neurons could indeed be induced to up-regulate expression of these proteins. Our results indicate again that two mutations within the S protein of HCoV-OC43 led to a different kinetics of induction of the UPR.

The IRE1/XBP1 pathway was differentially activated following infection of human neurons by the HCoV-OC43 rOC/U$_{S183-241}$ variant, as compared to infection with HCoV-OC43 wild type

The IRE1/XBP1 pathway was then studied to complete the portrait of the UPR induced in human neurons after infection with HCoV-OC43. Following its activation by ER stress, IRE1 induces an unconventional splicing of Xbp1(u) mRNA, producing the Xbp1(s) form lacking 26 nucleotides (Yoshida et al., 2001), which leads to translation of the transcriptional factor XBP1, that binds to ERSE, ERSE-II and UPR element (UPRE) (Yamamoto et al., 2004) within the
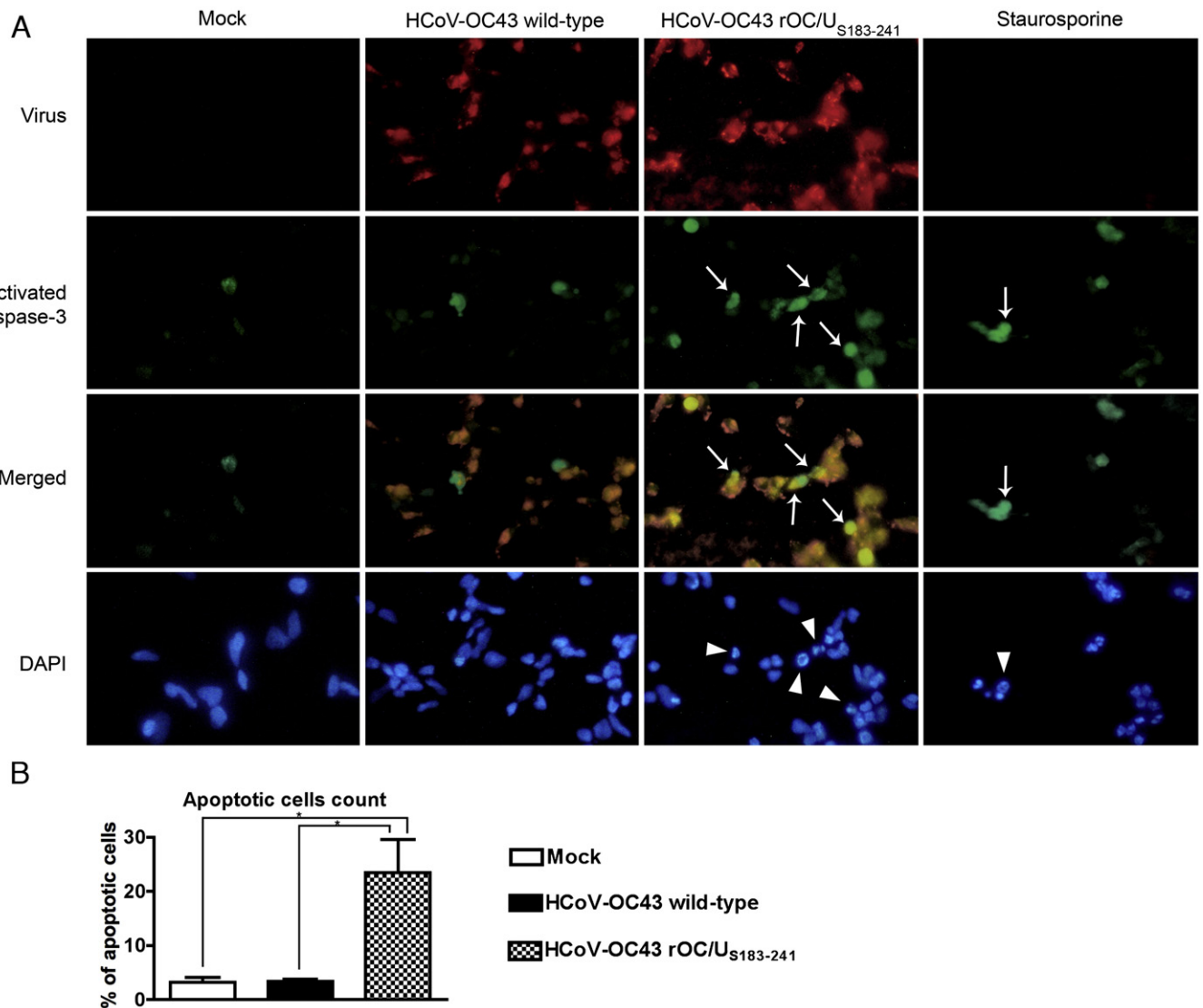

Fig. 8. Infection of human neurons by HCoV-OC43 rOC/U$_{S183-241}$ led to a strong activation of caspase-3 and nuclear fragmentation following strong UPR activation. Detection of activation of caspase-3 and nuclear fragmentation within neurons infected by HCoV-OC43 wild-type or HCoV-OC43 rOC/U$_{S183-241}$. (A) Immunofluorescence of LA-N-5 differentiated into human neurons infected with HCoV-OC43 wild-type or HCoV-OC43 rOC/U$_{S183-241}$ showing HCoV-OC43 S protein (red), caspase-3 activation (green), their colocalization in merged image (yellow) and nuclear fragmentation by DAPI (blue). Arrows indicate example of infected cells with activated caspase-3. Arrowheads show example of cells with intense fragmented nucleus. Staurosporine-treated samples served as a positive control. (B) Quantification of cells showing nuclear fragmentation. Data are presented as a percentage of cells with nuclear fragmentation compared to total cells in the field. Each quantification represents the mean of 5 fields containing at least 100 cells. Statistical significance: *p< 0.001.

promoter of a series of specific genes. Consequently, XBP1 is involved in the expression of ERAD-related genes, such as Edem and Herp (Kim et al., 2008; Olivari et al., 2006), chaperones such as Grp94 (Lee et al., 2003), and P58 ipk (Lee et al., 2003; van Huizen et al., 2003), an inhibitor of eIF2-alpha phosphorylation.

As our microarray results revealed a modulation of these four genes that are under the control of XBP1, the potential modulation of their expression was confirmed by quantitative PCR following infection by HCoV-OC43 wild-type and HCoV-OC43 rOC/$U_{S183-241}$ (Fig. 7A). Our results also showed clear differences in the kinetics of induction of these genes by the two viruses. Expression of the Edem, Herp, Grp94 and P58-ipk genes was induced within 24 h post-infection by HCoV-OC43 rOC/$U_{S183-241}$, and decreased at 72 h post-infection. On the other hand, HCoV-OC43 wild-type infection led to a continuous but lower increase over the course of infection, at least up to 72 h post-infection. This led us to assess the increase of Xbp1(s) mRNA by quantitative PCR, with primers spanning the 26-nucleotide intron (Hirota et al., 2006), and measure the increase of the Xbp1(s) mRNA concurrently to the decrease of the Xbp1(u) form by RT-PCR, with primers flanking the 26-nucleotide intron (Hirota et al., 2006) (Figs. 7A and B). Our results clearly showed a strong increase in the Xbp1(s) form at 24 and 48 h after infection by HCoV-OC43 rOC/$U_{S183-241}$, followed by a subsequent decrease. On the other hand, infection by HCoV-OC43 wild-type resulted in a constant but slower increase in the amount of Xbp1(s) form over the course of the infection, at least up to 72 h post-infection. The kinetics of Xbp1(u) cleavage correlated with the upregulation of expression of the four XBP1-controlled genes that we analyzed after infection by both viruses (Fig. 7A), and indicated an unambiguous activation of the IRE1/XBP1 pathway.

Moreover, Western blot analysis confirmed that the expression of the Grp94 gene, which can be under the control of XBP1, led to a significant increase in the amount of its corresponding protein within neurons following infection by HCoV-OC43 rOC/$U_{S183-241}$ (Fig. 7B). Thapsigargin-treated cells were used as a positive control to confirm that the LA-N-5 neurons could indeed be induced to express this protein. Altogether, our data demonstrate again that only two mutations within the S protein of HCoV-OC43 can lead to a different kinetics and amplitude of UPR activation.

Infections of human neurons by HCoV-OC43 rOC/$U_{S183-241}$ led to a strong activation of caspase-3 and nuclear fragmentation following a stronger UPR activation

Following the deciphering of the UPR induced by HCoV-OC43 wild-type and HCoV-OC43 rOC/$U_{S183-241}$, we investigated whether the latter could lead to increased neuronal death by apoptosis following a stronger UPR activation. Caspase-3 and nuclear fragmentation are hallmarks of apoptosis and were shown to be induced following virus-induced UPR (Medigeshi et al., 2007). We assayed the activation of caspase-3 by immunofluorescence at 48 h post-infection, a time where we observed the most significant differences in UPR activation and protein synthesis rate between the two viruses (Fig. 8). At 48 h post-infection, neurons infected by HCoV-OC43 wild-type did not exhibit significant differences in caspase-3 activation and nuclear fragmentation compared to mock-infected cells. In contrast, most of the neurons infected by HCoV-OC43 rOC/$U_{S183-241}$ showed intense activation of caspase-3, as well as nuclear fragmentation. Indeed, quantification of apoptotic cells support our conclusion that neurons
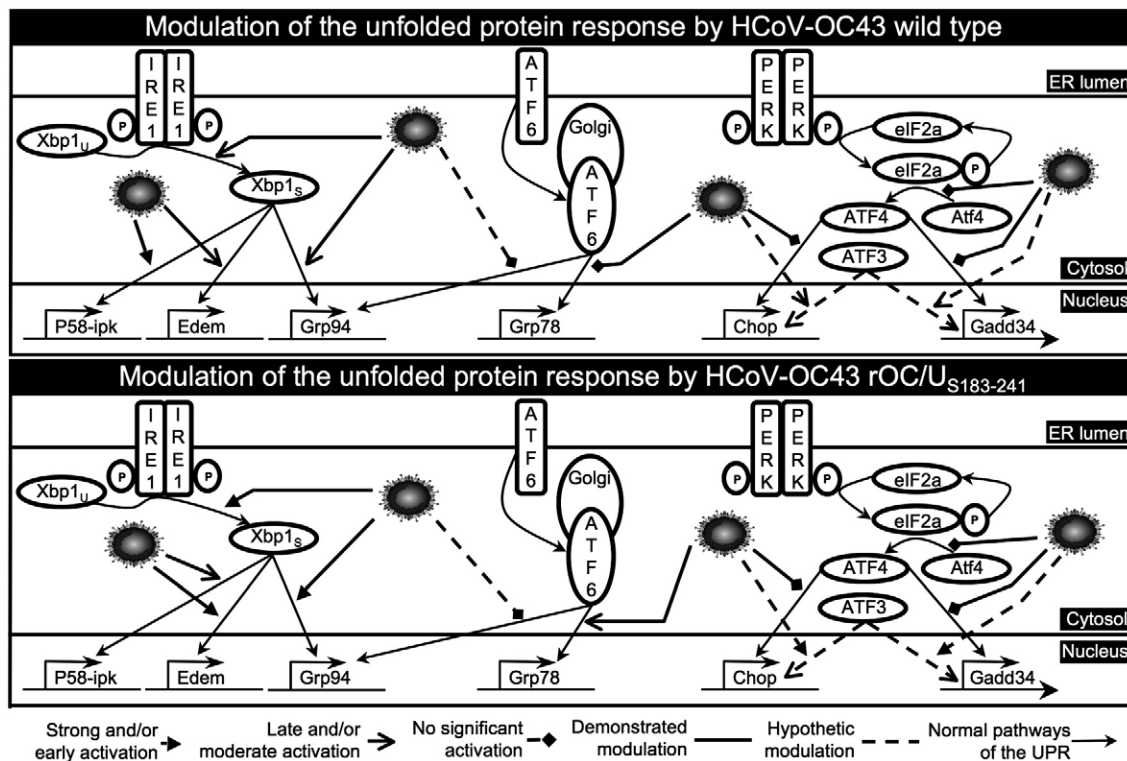

Fig. 9. Model depicting the activation of the normal UPR and possible modulation of the different pathways by the HCoV-OC43 S protein in human neuronal cells. The IRE1/XBP1 pathway is strongly and rapidly activated by the HCoV-OC43 rOC/$U_{S183-241}$ mutant while its activation is less intense and slower by HCoV-OC43 ATCC. Target genes of XBP1, e.g. Grp94, P58-ipk and Edem, are expressed following the appearance of the Xbp1$_S$ spliced form. The ATF6 pathway is thought to play a minor role, if any, in the UPR activated by both viruses. Indeed, its well known major target gene, Grp78, is merely expressed and no expression upregulation of the GRP78 protein is observed in both infection. The PERK/eIF2α pathway is only transiently activated by both viruses in the first 24 h post-infection although HCoV-OC43 rOC/$U_{S183-241}$ induced a strong translational protein shutoff starting at 48 h post-infection. However, no ATF4 protein was found during the course of infections by both viruses, even though Chop and Gadd34 gene were expressed. This could be explained by the expression of ATF3, also known to regulate their expression. Acronyms. IRE1: inositol-requiring enzyme 1; PERK: PKR-like ER kinase; ATF6: activating transcription factor 6; Xbp1$_U$: X-box binding protein mRNA unspliced form; Xbp1$_S$: X-box binding protein mRNA spliced form; ATF4: activating transcription factor 4; ATF3: activating transcription factor 3; eIF2α: α subunit of eukaryotic translation initiation factor 2.

infected by HCoV-OC43 rOC/U$_{S183-241}$ exhibited more nuclear fragmentation than mock-infected or HCoV-OC43-infected cells (Fig. 8B). Cells treated for 24 h with staurosporine, a common apoptosis inducer, served as a positive control. Moreover, cells experiencing intense activation of caspase-3 following HCoV-OC43 rOC/U$_{S183-241}$ infection were also positive for viral antigens and nuclear fragmentation. Altogether, our results showed that HCoV-OC43 rOC/U$_{S183-241}$ induced caspase-3 activation and nuclear fragmentation, two common apoptosis markers, as early as 48 h p.i., whereas HCoV-OC43 wild-type did not show any significant activation of either compared to mock-infected cells.

Discussion

The complete transcriptomic profile of human neurons infected by HCoV-OC43 revealed the modulation of expression of 275 genes among which many are known to be related to the activation of the UPR. Making use of a mutant virus harboring persistence-associated mutations in the S glycoprotein, we sought to evaluate the role of the HCoV-OC43 S protein on the UPR and neuronal viability. Altogether, our results demonstrate that only two point mutations in the S protein influence the activation of the UPR by HCoV-OC43 and shed light on the importance of discrete molecular determinants in the genome of HCoV-OC43 in the activation of the UPR in human neurons and induction of neuronal death.

Our results establish the relevance of two human neuronal models, NT2 and LA-N-5, to study early events occurring in human neurons following infection by HCoV-OC43. These cells are of particular interest since primary human neurons are difficult to obtain in sufficient quantity and quality for in vitro studies. Moreover, as coronaviruses, such as HCoV-OC43 and SARS-CoV, have been associated with neurological diseases in mice (Jacomy and Talbot, 2003; Netland et al., 2008) and potentially in humans (Arbour et al., 2000; Gu et al., 2005), these two neuronal models are useful to study the neuronal response to infection in the context of potential human neuropathologies.

Overall, our microarray results provide an overview of gene diversity associated with different molecular pathways that could be modulated in human neurons infected by a human coronavirus. Among the global transcriptomic modulation, several genes are associated with the translation machinery, neurotransmission, immunity and cytoskeleton factors. One important group of genes that attracted our attention was related to the biosynthesis and degradation functional group (Fig. 2) and more precisely associated with the process of the unfolded protein response (UPR), which has already been shown to be induced by other coronaviruses, such as MHV (Bechill et al., 2008) and SARS-CoV (Chan et al., 2006; Sung et al., 2009). Considering the numerous studies suggesting an association of neurological diseases with the activation of ER stress (Lindholm et al., 2006; Paschen, 2003), it is of importance to study the induction of the UPR in a human neuronal model by a virus which has been associated with neurological diseases (Arbour et al., 2000; Jacomy and Talbot, 2003).

The use of the HCoV-OC43 rOC/U$_{S183-241}$ variant is of high interest because the S protein of coronaviruses have been shown to induce the UPR (Chan et al., 2006; Versteeg et al., 2007) and especially since this variant has been shown to be more neurovirulent in mice (H. Jacomy and P. J. Talbot, submitted for publication). As clearly shown in Fig. 3, the comparison of infectious viral particles production between HCoV-OC43 wild-type and HCoV-OC43 rOC/U$_{S183-241}$ showed that both viruses bear the same capacity to produce extracellular infectious particles and that they disseminated in neuronal culture at the same rate. However, HCoV-OC43 rOC/U$_{S183-241}$ showed a more rapid and intense production of viral proteins and intracellular infectious viral particles. This suggests that discrete molecular viral S determinants could play a role in virus–cell interactions, leading to

an increased capacity to produce viral proteins and infectious viral particles. More importantly, the resulting increase in viral proteins present in the ER suggest that the cells might experience a more intense UPR activation in order to cope with an increased ER stress caused by the burden of viral proteins. Therefore, mutations in the S protein of HCoV-OC43, which lead to an increased neurovirulence in mice, induce a different kinetics of UPR activation. Considering that an uncontrolled UPR appears to be associated with neurological diseases (Lindholm et al., 2006; Paschen, 2003), we studied its level of activation following infection by HCoV-OC43 wild-type and HCV-OC43 rOC/U$_{S183-241}$ in human neurons, which are the main target of infection and determined whether these mutations could lead to increased neuronal death (Fig. 9).

We characterized the splicing of XBP1 as a standard analysis to identify the activation of the IRE1/XBP1 pathway (Fig. 7B) and found that HCoV-OC43 promoted the splicing of XBP1 and the expression of genes partially or solely under the control of this transcriptional factor (Fig. 7A). Indeed, we showed that HCoV-OC43 infection induced the upregulation of expression of a negative regulator of PERK and PKR activity, P58-ipk, and of a central gene in the ERAD complex, Edem, both solely under the control of XBP1 following activation of the UPR (Lee et al., 2003; Yamamoto et al., 2004). Altogether, these results indicate an unambiguous activation of the IRE1/XBP1 pathway following HCoV-OC43 infection. Indeed, the increase of Xbp1 splicing (Figs. 7A and B) directly correlated with the increased expression of these genes, thus reinforcing our hypothesis of activation of the IRE1/XBP1 pathway. Moreover, HCoV-OC43 rOC/U$_{S183-241}$ induced a more rapid and stronger splicing of Xbp1 mRNA, indicating an increased activation of the IRE1/XBP1 pathway by this virus variant compared to wild-type virus.

On the other hand, we only found a transient level of phosphorylated eIF2-alpha at 24 h post-infection (Fig. 5A), suggesting that the main effector of the PERK/eIF2-alpha pathway, ATF4, might not be efficiently translated following HCoV-OC43 infection, thus suggesting an ATF4-independent induction of the UPR. Moreover, we hypothesize that the increased expression of the cellular inhibitor of PERK P58-ipk, starting at 48 h post-infection, may help explain the absence of phosphorylation of eIF2-alpha at 48 and 72 h post-infection (Fig. 7A). However, even if we were not able to detect any ATF4 protein (Fig. 6B), we observed a significant upregulation of expression of the Gadd34 and Chop genes (Fig. 6A), which are largely considered to be under the control of ATF4. However, although ATF4 plays a major role in the expression of these genes, other factors are known to regulate their expression. ATF3 is a transcriptional factor that has been shown to regulate Gadd34 and Chop gene expression (Haneda et al., 2004; Jiang et al., 2004). Given that our microarray results showed an upregulation of the expression of ATF3 (data not shown), we hypothesize that Gadd34 and Chop might be induced by this transcriptional factor instead of ATF4. Furthermore, the expression of the Chop gene was also shown to be under the control of XBP1 (Lee et al., 2003), which correlates with our results (Figs. 6A, 7A and B). Considering our results showing upregulation of the Edem and P58-ipk genes, solely under XBP1 control (Lee et al., 2003), this adds to the possible involvement of XBP1 in the expression of Chop. The absence of expression of the CHOP protein is striking considering the strong upregulation of Chop mRNA by HCoV OC43 rOC/U$_{S183-241}$ (Fig. 6A). However, this may suggest a post-transcriptional regulation of the Chop gene in coronavirus infection, as it has already been shown for INF-beta by MHV (Roth-Cross et al., 2007). Altogether, our results indicate that the PERK/eIF2-alpha pathway does not play a significant role in the infection of neuronal cells by HCoV-OC43.

Although the level of phosphorylated eIF2-alpha was only transient, we did observe a translational shutoff after infection, particularly important for HCoV-OC43 rOC/U$_{S183-241}$ within 48 h of infection (Fig. 5B). It is of interest to consider that such attenuation of translation can occur concurrently with increased protein degradation

by the ERAD complex. The strong upregulation of Edem (Olivari et al., 2006) and Herp (Kim et al., 2008) gene expression (Fig. 6A), especially after HCoV-OC43 rOC/U$_{S183-241}$ infection might in part explain this phenomenon, as these proteins are associated with protein degradation during the UPR (Figs. 5B and C). Moreover, translational shutoff is a common hallmark preceding cell death, which was also already very strong at 48 h post-infection by the HCoV-OC43 rOC/U$_{S183-241}$ variant, as shown by a viability assay (Fig. 5D) and evaluation of apoptosis induction by caspase-3 activation and nuclear fragmentation (Figs. 8A and B). Thus, considering the strong upregulation of gene expression of Edem and Herp known for their role in protein degradation, the significant activation of caspase-3 and the induction of nuclear fragmentation, we hypothesize that the strong decrease in protein synthesis detected following HCoV-OC43 rOC/U$_{S183-241}$ infection might be the result of an increased protein degradation by the ERAD complex concurrently with initial activation steps of apoptosis.

While deciphering the UPR following a viral infection, one should bear in mind that redundancy between activated and non-activated pathways and compensating mechanisms for transcriptional gene control, may also lie elsewhere than within the three well-known UPR pathways. Indeed, such complex cross-talk between the UPR pathways using knock-out of XBP1 and ATF6 was reported (Lee et al., 2003). This would account for the expression of Grp94, which is under the control of both XBP1 and ATF6, following infection by HCoV-OC43 rOC/U$_{S183-241}$ at both mRNA and protein levels (Figs. 7A and B). Our results indicate that the expression of the Grp78 gene is slightly upregulated, but not to a significant level, as revealed by the absence of the corresponding protein in Western blot analysis (Figs. 4A and B). Interestingly, the knock-out of ATF6 or XBP1 alone was shown to induce a very weak loss of Grp78 expression, showing redundancy between these pathways (Lee et al., 2003). In contrast, other groups showed that XBP1 knock-out only slightly impaired Grp78 expression and that ATF6 is the major inductor of Grp78 (Yamamoto et al., 2004). However, further studies need to be performed in order to decipher the cross-talk between ATF6 and XBP1 pathways. Nevertheless, our results do suggest that the low level of expression of Grp78 mRNA could account for the XBP1 activity, as it weakly induces the ERSE promoter (Yamamoto et al., 2004), and that a full activation of the ATF6 pathway would have led to a strong GRP78 protein expression, as revealed by thapsigargin treatment (Fig. 4A). Therefore, we hypothesize that the ATF6 pathway plays a minor role, if any, in the UPR activated by HCoV-OC43, leading to the absence of upregulation of GRP78 protein and that consequently GRP94 protein expression is likely to account for XBP1 activity.

Our results showed that the HCoV-OC43 rOC/U$_{S183-241}$ variant harboring point mutations within its S protein can lead to an increased production of viral proteins and intracellular infectious viral particles and we speculate that these events could give rise to an increased ER stress leading to a stronger activation of the UPR (Fig. 9). Indeed, others have already shown that the S protein of MHV (Versteeg et al., 2007) and SARS-CoV (Chan et al., 2006) or the 8ab protein of SARS-CoV (Sung et al., 2009) can alone induce the UPR and that only the presence or accumulation of the protein is thought to be responsible for the ER stress (Versteeg et al., 2007). Our study clearly reveals that mutations within the S protein of HCoV-OC43 can differentially induce the UPR and lead to a stronger neuronal death by apoptosis, as shown by intense caspase-3 activation and nuclear fragmentation (Figs. 8A and B). Interestingly, IRE1 was linked to the JNK pathway that is involved in apoptosis following the UPR (Urano et al., 2000) and JNK activation can be modulated by other virus, such as HCMV, to cope with cell death (Xuan et al., 2009). One might speculate that the JNK pathway could play a role in the strong neuronal apoptosis induced by HCoV-OC43 rOC/U$_{S183-241}$, as we observed a strong and unambiguous activation of the IRE1/XBP1 pathway. Studies are currently underway to decipher the possible implication of the JNK pathway in our model.

In summary (Fig. 9), the present study demonstrates that only two point mutations within the S protein of HCoV-OC43, which are acquired upon persistence in human neural cells and lead to increased neurovirulence in mice (H. Jacomy and P. J. Talbot, submitted for publication), also lead to: (1) an increase in production of viral proteins and intracellular infectious viral particles; (2) a stronger and faster induction of the UPR (Fig. 9); (3) an increased attenuation of translation with only transient phosphorylation level of eIF2-alpha; and (4) an increased neuronal cell death by apoptosis. Moreover, it suggests that mutations of RNA viruses acquired during persistence in the central nervous system could modulate neuropathogenesis in the context of virus-mediated neurodegenerative diseases. Such studies are on-going in our animal model of human coronavirus neuropathogenesis.

Materials and methods

Cell lines, viruses, infection and thapsigargin treatment

The cell lines N-Tera2 (a gift from Dr. Glenn Rall, University of Pennsylvania School of Medicine) and LA-N-5 (a gift from Dr. Stephan Ladisch, George Washington University School of Medicine) were cultured in DMEM supplemented with 10% (v/v) fetal bovine serum (FBS) and RPMI supplemented with 15% (v/v) FBS, 10 mM HEPES, 1 mM sodium pyruvate and 100 μM non-essential amino acids (Gibco-Invitrogen), respectively. The N-Tera2 cells were differentiated into human neurons (NT2-N), as previously described (Pleasure and Lee, 1993). Briefly, 2×10^6 cells were seeded in a 75 cm^2 flask in DMEM medium supplemented with 10% (v/v) FBS. The next day, and every 3 days for 4 weeks, medium was replaced by the same medium also containing 10 μM all-trans retinoic-acid (Sigma). Cells were then trypsinized and plated into Petri dishes (1×10^7 cells) or 24-well (2×10^5) plates coated with poly-D-lysine (Sigma, P-1149) and matrigel (BD Biosciences) and cultured for 2 weeks with DMEM medium supplemented with 5% (v/v) FBS, 1 μM AraC, 10 μM FudR and 10 μM UriD (Sigma), with medium replaced every 3 days. The LA-N-5 cells were differentiated into human neurons as previously described (Hill and Robertson, 1998). Briefly, cells were seeded in Cell+Petri dishes (5×10^5 cells), 6-well (4×10^4 cells), 24-well (5×10^3 cells) or 96-well (1.8×10^3 cells) plates (Sarstedt), in RPMI medium supplemented with 10% (v/v) FBS, 10 mM HEPES, 1 mM sodium pyruvate and 100 μM non-essential amino acids. The next day, and every 2 days for 6 days, medium was replaced with the same medium also containing 10 μM all-trans retinoic-acid.

HCoV-OC43 was obtained several years ago from the American Type Culture Collection (ATCC VR-759) and propagated on the HRT-18 cell line as previously described (Mounir and Talbot, 1992). A recombinant HCoV-OC43 variant containing two point mutations within the S protein (H183R and Y241H), named HCoV-OC43 rOC/U$_{S183-241}$, was generated using the full-length cDNA clone pBAC-OC43^{FL}, as previously described (St-Jean et al., 2006). The genome of HCoV-OC43 rOC/U$_{S183-241}$ was completely sequenced to confirm that the only differences with the HCoV-OC43 ATCC VR-759 strain were the two inserted mutations in the S glycoprotein. Cells were infected at a MOI of 0.2 or mock-infected, then incubated at 37 °C for 2 h, washed with PBS and incubated at 37 °C with fresh medium. Cells and supernatants were harvested at the indicated times post-infection. Cells were treated with 2 μM thapsigargin, or 2 μM staurosporine or mock-treated and harvested at the indicated times.

Immunofluorescence

Cells were fixed with 4% (w/v) paraformaldehyde for 20 min at room temperature, permeabilized with methanol at −20 °C for 5 min, incubated with primary mouse monoclonal antibody (mAb) directed against β-tub isoform III (1/1000, Chemicon) and rabbit antiserum specific to BCoV, serologically related to HCoV-OC43 (undiluted) (gift

from the late Dr. Serge Dea, INRS-Institut Armand-Frappier), or incubated with rabbit polyclonal antibody NFM (1/100, Chemicon) or with rabbit polyclonal antibody to activated Caspase-3 (1/50, R and D Systems) and culture supernatant of mouse hybridoma containing mAb 1-10C.3 directed against the S protein of HCoV-OC43 (undiluted), or incubated only with mAb 1-10C.3 (1/100) for 1 h at room temperature and washed 3 times with PBS. Cells incubated with β-tub isoform III antibody and antiserum specific to BCoV were then incubated for 1 h at room temperature with two secondary antibodies (Molecular Probes-Invitrogen): anti-rabbit AlexaFluor568 (1/1000) and anti-mouse AlexaFluor488 (1/1500). Cells incubated with NFM antibody or activated Caspase-3 antibody and mAb 1-10C.3 were then incubated with the anti-mouse AlexaFluor568 (1/1000) and anti-rabbit AlexaFluor488 (1/1500) for 1 h at room temperature. Cells incubated with only mAb 1-10C.3 were then incubated with the anti-mouse AlexaFluor568 (1/1000) for 1 h at room temperature. All cells were then incubated with DAPI for 5 min and then washed three times with PBS prior to imaging. ANOVA tests followed by *post-hoc* Tukey's analysis were performed to determine the statistical significance of the differences in number of cells showing fragmented nuclei between samples, using SPSS software version 16.

RNA isolation, quantitative real-time PCR and microarray experiments

Total RNA was extracted at 24, 48 and 72 h post-infection using the Agilent RNA extraction kit according to the manufacturer's instructions, quantified using a ND1000 spectrophotometer (Nanodrop) and RNA integrity assessed by microfluidic electrophoresis using the Agilent RNA 6000 Nano kit with the Agilent 2100 Bioanalyzer. Microarray experiments were performed using the Low RNA Input linear amplification kit (Agilent) (Zhu et al., 2006), according to the manufacturer's protocol, where CTP-Cy3 (Perkin-Elmer) and CTP-Cy5 (Perkin-Elmer) were incorporated into cRNA. Equimolar solution of cRNA from infected and mock-infected cells were hybridized for 17 h at 65 °C on the Agilent 60-mer Oligo Microarray Human 1A v2, 22K chip, which represents 22,000 human transcripts. Microarray fluorescence was revealed using a ProScanArray HT scanner (Perkin-Elmer) at a 5 μm resolution and colorimetric intensity quantified using the ProScanArray Express software (Perkin-Elmer). Statistics were performed with the open-source software Microarray Data Analysis System (MIDAS) from the TM4 microarray software suite (Saeed et al., 2003), using combined threshold for a significant gene modulation of $p < 0.05$ and a minimum of 2-fold modulation of expression in two independent viral infections. Transcriptomics time-point analysis was made from two independent infections, where each of the time-point was performed in dye-swap quadruplicate. cDNAs for quantitative real-time PCR were obtained from total RNA extracts reverse-transcribed using the SuperscriptII first-strand kit with oligo-dT primers (Invitrogen), according to the manufacturer's protocol. Real-time quantitative PCR was performed using the DyNAmo SYBR green qPCR kit (NEB) with the Rotor-gene 3000 (Corbett Life Science) with 1 cycle of 95 °C for 15 min, followed by 40 cycles at 94 °C for 30 s, 60 °C for 30 s, and 72 °C for 30 s. Modulation of gene expression from quantitative real-time PCR was analyzed using the $2^{-\Delta\Delta Ct}$ method (Livak and Schmittgen, 2001) and normalized to Gapdh expression. ANOVA tests followed by *post-hoc* Tahame's analysis were performed to determine the statistical significance of the differences in gene expression between samples, using SPSS software version 16.0. Primers used are presented in supplementary data.

Protein extraction and immunoblotting

Total protein was extracted using RIPA buffer (150 mM NaCl, 50 mM Tris, pH 7.4, 1% (v/v) NP-40, 0.25% (w/v) sodium deoxycholate, 1 mM EDTA) supplemented with the Protease cocktail

inhibitor (Sigma) and the Halt-Phosphatase inhibitor (Pierce). Harvested cells were vortexed for 1 min into RIPA buffer, incubated on ice for 20 min, centrifuged for 5 min at 4 °C at 17,000×g and supernatants were stored at −80 °C until further analyzed. Protein concentration was determined using the BCA Protein assay kit (Novagen), according to the manufacturer's protocol. Equal amounts of protein were subjected to SDS-PAGE using a 10% or 4–12% gradient gel Novex NuPage (Invitrogen), transferred to PVDF membrane (Millipore) with the Bio-Rad Semi-dry transblot apparatus. Membranes were blocked overnight at 4 °C with TBS buffer containing 1% (v/v) Tween (TBS-T) and 5% (w/v) non-fat milk, then incubated with rabbit anti-ATF4 antibody (1/200, SantaCruz), mouse anti-CHOP antibody (1/200, SantaCruz), rabbit anti-total eIF2-alpha antibody (1/1000, Cell Signaling), rabbit anti-phosphorylated Ser52-eIF2-alpha antibody (1/1000, BioSource), rabbit anti-GADD34 antibody (1/250, SantaCruz), mouse anti-GAPDH antibody (1/5000, Chemicon), mouse anti-GRP78 antibody (1/1000, BD Biosciences) or rabbit anti-GRP94 antibody (1/1000, Stressgen) for 1 h at room temperature. After TBS-T washes, the membranes were incubated with secondary antibody anti-mouse or anti-rabbit, coupled to horseradish peroxidase (GE Life Sciences) and detection made by chemiluminescence using the ECL kit (GE Life Sciences) using Kodak-XOmat L-S film (Kodak).

Radiolabeling

Cell cultures were starved in cystein-and methionine-free medium for 30 min, incubated with 70 μCi of ^{35}S-radiolabeled cystein/methionine using the EXPRE^{35}S^{35}S protein labeling mix (Perkin-Elmer) for 15 min, washed twice with ice-cold PBS buffer and harvested. Proteins were extracted with RIPA buffer, as described above. Equal volumes of whole cell extracts were precipitated in triplicate using the trichloroacetic acid technique and assayed for cpm counts using a Beckman LS1701 scintillation counter, or subjected to SDS PAGE using 4–12% gradient gel Novex NuPage (Invitrogen), fixed with 30% (v/v) glacial acetic acid and 10% (v/v) methanol solution for 30 min, incubated in Kodak Enlightning Rapid Autoradiography Enhancer (Perkin-Elmer) for 30 min and exposed at −80 °C using Kodak-XOmat L-S film. ANOVA tests followed by *post-hoc* Tahame's analysis were performed to determine the statistical significance of the differences in cpm counts between samples, using SPSS software version 16.0.

Cell viability assay

Viability was assayed by the reduction of 3-[4,5,dimethylthiazol-2-yl]-5-[3-carboxyme thoxy-phenyl]-2-[4-sulfophenyl]-2H-tetrazolium, inner salt (MTS) in the presence of phenazine methosulfate (PMS), as previously described (Cory et al., 1991). Briefly, infected, mock-infected, thapsigargin-treated and mock-treated cells, cultured in 96-well plates, were incubated in the presence of 0.6 mM MTS (Promega) and 14 μM PMS (Sigma-Aldrich) at 24, 48 or 72 h post-infection and absorbance was read at 492 nm every 20 min for 3 h. Viability was determined by slope regression analysis for each sample and is expressed as a relative percentage compared to mock-infected cells slope. Student's t test was performed to determine the statistical significance of the differences in slope between samples, using SPSS software version 16.0.

Flow cytometry

Cells were harvested at 4, 16 and 24 h post-infection and 4×10^6 cells were fixed and permeabilized with methanol at −20 °C for 5 min. After 2 washes with PBS, cells were incubated with 100 μl (5 μg) of culture supernatant of mouse hybridoma containing mAb 1-10C.3 directed against the S protein of HCoV-OC43, or with 100 μl (5 μg) culture supernatant of mouse hybridoma containing mAb 5–

11 H.6 directed against the S protein of HCoV-229E as an isotype control, or with 100 μl of PBS for 1 h at room temperature. Cells were then washed three times with PBS and incubated with secondary antibody anti-mouse AlexaFluor488 (1/500) for 1 h at room temperature. Cells were then washed three times and analyzed using a FACS calibur cytofluorometer. Data analysis was performed using Cell Quest Pro (BD Bioscience). ANOVA tests followed by *post-hoc* Tahame's analysis were performed to determine the statistical significance of the differences in the percentage of infected cells between samples, using SPSS software version 16.0.

Microarray data

Whole transcriptomics data issued from microarray experiments are deposited and available in the public database GEO at http://www.ncbi.nlm.nih.gov/projects/geo/.

Acknowledgments

Appendix A. Supplementary data

Supplementary data associated with this article can be found, in the online version, at doi:10.1016/j.virol.2009.09.026.

References

Antony, J.M., Ellestad, K.K., Hammond, R., Imaizumi, K., Mallet, F., Warren, K.G., Power, C., 2007. The human endogenous retrovirus envelope glycoprotein, syncytin-1, regulates neuroinflammation and its receptor expression in multiple sclerosis: a role for endoplasmic reticulum chaperones in astrocytes. J. Immunol. 179, 1210–1224.

Arbour, N., Côté, G., Lachance, C., Tardieu, M., Cashman, N.R., Talbot, P.J., 1999. Acute and persistent infection of human neural cell lines by human coronavirus OC43. J. Virol. 73, 3338–3350.

Arbour, N., Day, R., Newcombe, J., Talbot, P.J., 2000. Neuroinvasion by human respiratory coronaviruses. J. Virol. 74, 8913–8921.

Bechill, J., Chen, Z., Brewer, J.W., Baker, S.C., 2008. Coronavirus infection modulates the unfolded protein response and mediates sustained translational repression. J. Virol. 82, 4492–4501.

Bonavia, A., Arbour, N., Yong, V.W., Talbot, P.J., 1997. Infection of primary cultures of human neural cells by human coronaviruses 229E and OC43. J. Virol. 71, 800–806.

Buchmeier, M.J., Dalziel, R.G., Koolen, M.J., Lampert, P.W., 1987. Molecular determinants of CNS virulence of MHV-4. Adv. Exp. Med. Biol. 218, 287–295.

Chan, C.P., Siu, K.L., Chin, K.T., Yuen, K.Y., Zheng, B., Jin, D.Y., 2006. Modulation of the unfolded protein response by the severe acute respiratory syndrome coronavirus spike protein. J. Virol. 80, 9279–9287.

Cheng, G., Feng, Z., He, B., 2005. Herpes simplex virus 1 infection activates the endoplasmic reticulum resident kinase PERK and mediates eIF-2alpha dephosphorylation by the gamma(1)34.5 protein. J. Virol. 79, 1379–1388.

Cory, A.H., Owen, T.C., Barltrop, J.A., Cory, J.G., 1991. Use of an aqueous soluble tetrazolium/formazan assay for cell growth assays in culture. Cancer Commun. 3, 207–212.

Gu, J., Gong, E., Zhang, B., Zheng, J., Gao, Z., Zhong, Y., Zou, W., Zhan, J., Wang, S., Xie, Z., Zhuang, H., Wu, B., Zhong, H., Shao, H., Fang, W., Gao, D., Pei, F., Li, X., He, Z., Xu, D., Shi, X., Anderson, V.M., Leong, A.S., 2005. Multiple organ infection and the pathogenesis of SARS. J. Exp. Med. 202, 415–424.

Haneda, M., Xiao, H., Hasegawa, T., Kimura, Y., Nakashima, I., Isobe, K., 2004. Regulation of mouse GADD34 gene transcription after DNA damaging agent methylmethane sulfonate. Gene 336, 139–146.

Harding, H.P., Novoa, I., Zhang, Y., Zeng, H., Wek, R., Schapira, M., Ron, D., 2000. Regulated translation initiation controls stress-induced gene expression in mammalian cells. Mol. Cell 6, 1099–1108.

Hill, D.P., Robertson, K.A., 1998. Differentiation of LA-N-5 neuroblastoma cells into cholinergic neurons: methods for differentiation, immunohistochemistry and reporter gene introduction. Brain Res. Brain Res. Protoc. 2, 183–190.

Hirota, M., Kitagaki, M., Itagaki, H., Aiba, S., 2006. Quantitative measurement of spliced XBP1 mRNA as an indicator of endoplasmic reticulum stress. J. Toxicol. Sci. 31, 149–156.

Imai, Y., Soda, M., Takahashi, R., 2000. Parkin suppresses unfolded protein stress-induced cell death through its E3 ubiquitin–protein ligase activity. J. Biol. Chem. 275, 35661–35664.

Imaizumi, K., Miyoshi, K., Katayama, T., Yoneda, T., Taniguchi, M., Kudo, T., Tohyama, M., 2001. The unfolded protein response and Alzheimer's disease. Biochim. Biophys. Acta 1536, 85–96.

Isler, J.A., Maguire, T.G., Alwine, J.C., 2005. Production of infectious human cytomegalovirus virions is inhibited by drugs that disrupt calcium homeostasis in the endoplasmic reticulum. J. Virol. 79, 15388–15397.

Jacomy, H., Talbot, P.J., 2003. Vacuolating encephalitis in mice infected by human coronavirus OC43. Virology 315, 20–33.

Jacomy, H., Fragoso, G., Almazan, G., Mushynski, W.E., Talbot, P.J., 2006. Human coronavirus OC43 infection induces chronic encephalitis leading to disabilities in BALB/C mice. Virology 349, 335–346.

Jiang, H.Y., Wek, S.A., McGrath, B.C., Lu, D., Hai, T., Harding, H.P., Wang, X., Ron, D., Cavener, D.R., Wek, R.C., 2004. Activating transcription factor 3 is integral to the eukaryotic initiation factor 2 kinase stress response. Mol. Cell Biol. 24, 1365–1377.

Kim, T.Y., Kim, E., Yoon, S.K., Yoon, J.B., 2008. Herp enhances ER-associated protein degradation by recruiting ubiquilins. Biochem. Biophys. Res. Commun. 369, 741–746.

Lee, A.H., Iwakoshi, N.N., Glimcher, L.H., 2003. XBP-1 regulates a subset of endoplasmic reticulum resident chaperone genes in the unfolded protein response. Mol. Cell Biol. 23, 7448–7459.

Lindholm, D., Wootz, H., Korhonen, L., 2006. ER stress and neurodegenerative diseases. Cell Death Differ 13, 385–392.

Livak, K.J., Schmittgen, T.D., 2001. Analysis of relative gene expression data using real-time quantitative PCR and the 2(-Delta Delta C(T)) Method. Methods 25, 402–408.

Matsumoto, M., Minami, M., Takeda, K., Sakao, Y., Akira, S., 1996. Ectopic expression of CHOP (GADD153) induces apoptosis in M1 myeloblastic leukemia cells. FEBS Lett. 395, 143–147.

Medigeshi, G.R., Lancaster, A.M., Hirsch, A.J., Briese, T., Lipkin, W.I., Defilippis, V., Fruh, K., Mason, P.W., Nikolich-Zugich, J., Nelson, J.A., 2007. West Nile virus infection activates the unfolded protein response, leading to CHOP induction and apoptosis. J. Virol. 81, 10849–10860.

Mounir, S., Talbot, P.J., 1992. Sequence analysis of the membrane protein gene of human coronavirus OC43 and evidence for O-glycosylation. J. Gen. Virol. 73, 2731–2736.

Netland, J., Meyerholz, D.K., Moore, S., Cassell, M., Perlman, S., 2008. Severe acute respiratory syndrome coronavirus infection causes neuronal death in the absence of encephalitis in mice transgenic for human ACE2. J. Virol. 82, 7264–7275.

Novoa, I., Zeng, H., Harding, H.P., Ron, D., 2001. Feedback inhibition of the unfolded protein response by GADD34-mediated dephosphorylation of eIF2alpha. J. Cell Biol. 153, 1011–1022.

Okada, T., Yoshida, H., Akazawa, R., Negishi, M., Mori, K., 2002. Distinct roles of activating transcription factor 6 (ATF6) and double-stranded RNA-activated protein kinase-like endoplasmic reticulum kinase (PERK) in transcription during the mammalian unfolded protein response. Biochem. J. 366, 585–594.

Olivari, S., Cali, T., Salo, K.E., Paganetti, P., Ruddock, L.W., Molinari, M., 2006. EDEM1 regulates ER-associated degradation by accelerating de-mannosylation of folding-defective polypeptides and by inhibiting their covalent aggregation. Biochem. Biophys. Res. Commun. 349, 1278–1284.

Paschen, W., 2001. Dependence of vital cell function on endoplasmic reticulum calcium levels: implications for the mechanisms underlying neuronal cell injury in different pathological states. Cell. Calcium 29, 1–11.

Paschen, W., 2003. Endoplasmic reticulum: a primary target in various acute disorders and degenerative diseases of the brain. Cell. Calcium 34, 365–383.

Phillips, J.J., Chua, M.M., Lavi, E., Weiss, S.R., 1999. Pathogenesis of chimeric MHV4/MHV-A59 recombinant viruses: the murine coronavirus spike protein is a major determinant of neurovirulence. J. Virol. 73, 7752–7760.

Pleasure, S.J., Lee, V.M., 1993. NTera 2 cells: a human cell line which displays characteristics expected of a human committed neuronal progenitor cell. J. Neurosci. Res. 35, 585–602.

Ron, D., Walter, P., 2007. Signal integration in the endoplasmic reticulum unfolded protein response. Nat. Rev., Mol. Cell. Biol. 8, 519–529.

Roth-Cross, J.K., Martinez-Sobrido, L., Scott, E.P., Garcia-Sastre, A., Weiss, S.R., 2007. Inhibition of the alpha/beta interferon response by mouse hepatitis virus at multiple levels. J. Virol. 81, 7189–7199.

Saeed, A.I., Sharov, V., White, J., Li, J., Liang, W., Bhagabati, N., Braisted, J., Klapa, M., Currier, T., Thiagarajan, M., Sturn, A., Snuffin, M., Rezantsev, A., Popov, D., Ryltsov, A., Kostukovich, E., Borisovsky, I., Liu, Z., Vinsavich, A., Trush, V., Quackenbush, J., 2003. TM4: a free, open-source system for microarray data management and analysis. BioTechniques 34, 374–378.

Shi, Y., Vattem, K.M., Sood, R., An, J., Liang, J., Stramm, L., Wek, R.C., 1998. Identification and characterization of pancreatic eukaryotic initiation factor 2 alpha-subunit kinase, PEK, involved in translational control. Mol. Cell. Biol. 18, 7499–7509.

St-Jean, J.R., Desforges, M., Almazan, F., Jacomy, H., Enjuanes, L., Talbot, P.J., 2006. Recovery of a neurovirulent human coronavirus OC43 from an infectious cDNA clone. J. Virol. 80, 3670–3674.

Sung, S.C., Chao, C.Y., Jeng, K.S., Yang, J.Y., Lai, M.M., 2009. The 8ab protein of SARS-CoV is a luminal ER membrane-associated protein and induces the activation of ATF6. Virology 387, 402–413.

Talbot, P.J., Jacomy, H., Desforges, M., 2008. Pathogenesis of human coronaviruses other than severe acute respiratory syndrome coronavirus. In: Perlman, S., Gallagher, T., Snijder, E.J. (Eds.), Nidoviruses. ASM Press, Washington, D.C., pp. 313–324.

Tardif, K.D., Mori, K., Siddiqui, A., 2002. Hepatitis C virus subgenomic replicons induce endoplasmic reticulum stress activating an intracellular signaling pathway. J. Virol. 76, 7453–7459.

Tirasophon, W., Welihinda, A.A., Kaufman, R.J., 1998. A stress response pathway from the endoplasmic reticulum to the nucleus requires a novel bifunctional protein kinase/endoribonuclease (Ire1p) in mammalian cells. Genes Dev. 12, 1812–1824.

Tirasophon, W., Lee, K., Callaghan, B., Welihinda, A., Kaufman, R.J., 2000. The endoribonuclease activity of mammalian IRE1 autoregulates its mRNA and is required for the unfolded protein response. Genes Dev. 14, 2725–2736.

Tseng, G.C., Oh, M.K., Rohlin, L., Liao, J.C., Wong, W.H., 2001. Issues in cDNA microarray analysis: quality filtering, channel normalization, models of variations and assessment of gene effects. Nucleic Acids Res. 29, 2549–2557.

Umareddy, I., Pluquet, O., Wang, Q.Y., Vasudevan, S.G., Chevet, E., Gu, F., 2007. Dengue virus serotype infection specifies the activation of the unfolded protein response. Virol. J. 4, 91.

Urano, F., Wang, X., Bertolotti, A., Zhang, Y., Chung, P., Harding, H.P., Ron, D., 2000. Coupling of stress in the ER to activation of JNK protein kinases by transmembrane protein kinase IRE1. Science 287, 664–666.

van Huizen, R., Martindale, J.L., Gorospe, M., Holbrook, N.J., 2003. P58IPK, a novel endoplasmic reticulum stress-inducible protein and potential negative regulator of eIF2alpha signaling. J. Biol. Chem. 278, 15558–15564.

Versteeg, G.A., van de Nes, P.S., Bredenbeek, P.J., Spaan, W.J., 2007. The coronavirus spike protein induces endoplasmic reticulum stress and upregulation of intracellular chemokine mRNA concentrations. J. Virol. 81, 10981–10990.

Williams, B.L., Lipkin, W.I., 2006. Endoplasmic reticulum stress and neurodegeneration in rats neonatally infected with Borna disease virus. J. Virol. 80, 8613–8626.

Xuan, B., Qian, Z., Torigoi, E., Yu, D., 2009. Human cytomegalovirus protein pUL38 induces ATF4 expression, inhibits persistent JNK phosphorylation, and suppresses endoplasmic reticulum stress-induced cell death. J. Virol. 83, 3463–3474.

Yamamoto, K., Yoshida, H., Kokame, K., Kaufman, R.J., Mori, K., 2004. Differential contributions of ATF6 and XBP1 to the activation of endoplasmic reticulum stress-responsive cis-acting elements ERSE, UPRE and ERSE-II. J. Biochem. 136, 343–350.

Yeh, E.A., Collins, A., Cohen, M.E., Duffner, P.K., Faden, H., 2004. Detection of coronavirus in the central nervous system of a child with acute disseminated encephalomyelitis. Pediatrics 113, e73–e76.

Yoshida, H., Matsui, T., Yamamoto, A., Okada, T., Mori, K., 2001. XBP1 mRNA is induced by ATF6 and spliced by IRE1 in response to ER stress to produce a highly active transcription factor. Cell 107, 881–891.

Yu, C.Y., Hsu, Y.W., Liao, C.L., Lin, Y.L., 2006. Flavivirus infection activates the XBP1 pathway of the unfolded protein response to cope with endoplasmic reticulum stress. J. Virol. 80, 11868–11880.

Zhu, B., Xu, F., Baba, Y., 2006. An evaluation of linear RNA amplification in cDNA microarray gene expression analysis. Mol. Genet. Metab. 87, 71–79.

Zinszner, H., Kuroda, M., Wang, X., Batchvarova, N., Lightfoot, R.T., Remotti, H., Stevens, J.L., Ron, D., 1998. CHOP is implicated in programmed cell death in response to impaired function of the endoplasmic reticulum. Genes Dev. 12, 982–995.